

See discussions, stats, and author profiles for this publication at: <https://www.researchgate.net/publication/44574254>

Interaction Electric Hyperpolarizability Effects in Weakly Bound H₂O···Rg (Rg = He, Ne, Ar, Kr and Xe) Complexes †

ARTICLE in THE JOURNAL OF PHYSICAL CHEMISTRY A · MAY 2010

Impact Factor: 2.69 · DOI: 10.1021/jp101718s · Source: PubMed

CITATIONS

24

READS

100

2 AUTHORS, INCLUDING:



George Maroulis

University of Patras

237 PUBLICATIONS 4,320 CITATIONS

SEE PROFILE

Interaction Electric Hyperpolarizability Effects in Weakly Bound H₂O···Rg (Rg = He, Ne, Ar, Kr and Xe) Complexes[†]

Anastasios Haskopoulos and George Maroulis*

Department of Chemistry, University of Patras, GR-26500 Patras, Greece

Received: February 25, 2010; Revised Manuscript Received: April 17, 2010

We report an extensive high-level ab initio theoretical investigation of the interaction electric properties of the weakly bound complexes of water with rare gases, H₂O···Rg (Rg = He, Ne, Ar, Kr and Xe). Our approach relies on finite-field many-body perturbation theory (MP) and coupled-cluster (CC) calculations with flexible, carefully designed basis sets of Gaussian-type functions (GTFs). We have obtained estimates of the electron correlation effects on the reference self-consistent field (SCF) values at all levels of theory employed in this work. For the planar equilibrium configuration (*C_s* symmetry) of the complexes, at the CCSD(T) level of theory, the interaction mean first hyperpolarizability is positive (SCF values in parentheses): $\bar{\beta}_{\text{int}}/e^3a_0^3E_{\text{h}}^{-2}(\text{H}_2\text{O}-\text{Rg}) = 0.72(0.56), 1.20(0.79), 7.04(4.28), 9.88(5.34), \text{ and } 15.52(6.68)$ for Rg = He, Ne, Ar, Kr, and Xe, respectively. For the interaction mean second hyperpolarizability, we have obtained (SCF values in parentheses): $\bar{\gamma}_{\text{int}}/e^4a_0^4E_{\text{h}}^{-3}(\text{H}_2\text{O}-\text{Rg}) = -18.93(-14.19), -37.78(-24.35), -83.16(-72.42), -102.92(-125.70), \text{ and } -206.45(-286.83)$ for Rg = He, Ne, Ar, Kr, and Xe. In addition to the equilibrium values of the interaction electric properties, we have also extracted information for their dependence on the variation of the distance of the rare gas atom from the center of mass of the water molecule (without changing direction). The gradient of the interaction mean second hyperpolarizability at the equilibrium configuration is determined as $(d\bar{\gamma}_{\text{int}}/dR)_e/e^4a_0^3E_{\text{h}}^{-3}(\text{H}_2\text{O}-\text{Rg}) = 9.89(\text{He}), 25.42(\text{Ne}), 73.71(\text{Ar}), 144.71(\text{Kr}), \text{ and } 324.68(\text{Xe})$.

Introduction

The aggregation of water molecules and the structure, energetics, and physicochemical properties of water clusters^{1–4} and liquid water^{5,6} is a field of intense activity in recent years. Significant work has been reported on the electric dipole moment and the dipole (hyper)polarizability of water clusters,^{7–15} ice,^{16,17} and the water molecule in condensed phases.^{18–23} The intermolecular interactions of water clusters have attracted considerably less attention. In this work we focus on the interaction-induced electric dipole moment (μ), static polarizability (α), and first (β) and second (γ) dipole hyperpolarizability of H₂O–Rg complexes, Rg = He, Ne, Ar, Kr and Xe. The interaction-induced properties offer valuable information on the distortion of the molecule in real environments.²⁴ They are a key ingredient in collision- and interaction-induced spectroscopy.²⁵ Interaction-induced dipole moment and polarizability are routinely associated with large classes of phenomena as collision-induced absorption (CIA) and collision-induced light scattering (CILS).²⁶ More recently, there is active interest in interaction-induced hyperpolarizability due to the systematic exploration of collision-induced hyper-Rayleigh (CIHR) scattering in model systems as Ne–Ar,²⁷ Kr–Xe,²⁸ He–Ne,²⁹ He–Ar,³⁰ H₂–He,³¹ and H₂–Ar.³² We also mention significant recent work on the determination of the interaction-induced properties of CO–Ne³³ and CO–Ar³⁴ and their subsequent use for the determination of important physicochemical properties.

The theoretical prediction of the electric hyperpolarizability is a highly nontrivial task. Additional difficulties are present in the determination of the interaction (hyper)polarizability where

the quantities of interest are much smaller in magnitude than the respective properties of the interacting subsystems. We lean heavily on previous experience with H₂–H₂, Ne–HF, Ne–FH, He–He, Ne–Ne, Ar–Ar, and Kr–Kr,³⁵ Rg–CO₂,³⁶ Ne–Ar,³⁷ Xe₂,³⁸ Kr–Xe,³⁹ and He–H₂⁴⁰ (see also refs 29, 30, and 32). The most stable configuration of all systems studied in this work is of *C_s* symmetry. All systems are planar. For H₂O–Rg (Rg = He, Ne, and Ar) we have used the findings of other authors. For H₂O–Rg (Rg = Kr and Xe) we have calculated the potential energy surface (PES) in order to determine the respective minima. In addition to the interaction properties pertaining to the PES minima, we have obtained information for their dependence on the displacement of the Rg atom around the equilibrium position. We have explored in some depth important computational aspects as basis set effects and the relative merit of the quantum chemical methods employed in this work.

Our approach to the calculation of the interaction electric properties relies on the finite-field method.⁴¹ Essential computational details of our methodology may be found in previous work.^{42,43}

Theory

The energy (E^0) of an uncharged molecule in a weak, homogeneous electric field can be expanded as^{44,45}

$$E^0 = \mu_{\alpha} F_{\alpha} - (1/2)\alpha_{\alpha\beta} F_{\alpha} F_{\beta} - (1/6)\beta_{\alpha\beta\gamma} F_{\alpha} F_{\beta} F_{\gamma} - (1/24)\gamma_{\alpha\beta\gamma\delta} F_{\alpha} F_{\beta} F_{\gamma} F_{\delta} + \dots \quad (1)$$

F_{α} is the field, E^0 is the energy of the free molecule and the expansion coefficients (in bold) are, the dipole moment (μ_{α}), the dipole polarizability ($\alpha_{\alpha\beta}$), the first dipole hyperpolarizability

[†] Part of the “Klaus Ruedenberg Festschrift”.

* To whom all correspondence should be addressed. E-mail: maroulis@upatras.gr.

($\beta_{\alpha\beta\gamma}$), and the second dipole hyperpolarizability ($\gamma_{\alpha\beta\gamma\delta}$). A repeated subscript implies summation over x , y , and z . The number of independent components needed to specify the respective electric property tensors is strictly regulated by symmetry. We closely follow Buckingham's conventions and notation (see above-cited review). In the molecular orientation adopted in this work, H₂O is on the xz plane with its center of mass on the origin and the oxygen nucleus on the negative z axis. For a molecule of C_s symmetry, there are two independent components for the dipole moment, four for the dipole polarizability, six for the first, and nine for the second hyperpolarizability. The total dipole moment is defined by

$$\mu = (\mu_x^2 + \mu_z^2)^{1/2} \quad (2)$$

For the mean and the anisotropy of the dipole polarizability we have

$$\begin{aligned} \bar{\alpha} &= (\alpha_{xx} + \alpha_{yy} + \alpha_{zz})/3 \\ \Delta\alpha &= 2^{1/2}[(\alpha_{xx} - \alpha_{yy})^2 + (\alpha_{yy} - \alpha_{zz})^2 + (\alpha_{zz} - \alpha_{xx})^2 + 6\alpha_{xz}^2]^{1/2} \end{aligned} \quad (3)$$

The mean first dipole hyperpolarizability along the direction of the dipole moment, defined by the unit vector ($\mu_x/\mu, \mu_z/\mu$), is given by

$$\beta = (3/5)(\beta_x\mu_x + \beta_z\mu_z)/\mu \quad (4)$$

where $\beta_x = \beta_{xxx} + \beta_{xyy} + \beta_{xzz}$ and $\beta_z = \beta_{xxz} + \beta_{yyz} + \beta_{zzz}$.

Finally, the mean second hyperpolarizability is obtained as

$$\bar{\gamma} = (\gamma_{xxxx} + \gamma_{yyyy} + \gamma_{zzzz} + 2\gamma_{xxyy} + 2\gamma_{yyzz} + 2\gamma_{zzxx})/5 \quad (5)$$

We rely on flexible basis sets of Gaussian-type functions in order to obtain reliable, self-consistent field (SCF) results of near-Hartree–Fock quality. Electron correlation effects were estimated via Møller–Plesset perturbation theory (MP) and coupled-cluster (CC) techniques. Extensive presentations of these methods are available in standard textbooks^{46,47} and comprehensive reviews.^{48–51} In summary, the methods used in this work are as follows:

SCF, self-consistent-field

MP2, second-order, and

MP4, fourth-order Møller–Plesset perturbation theory

CCSD, singles and doubles coupled cluster, and

CCSD(T), which includes an estimate of connected triples via a perturbational treatment. The method with the highest predictive potential is, presumably, CCSD(T). The CCSD method is considerably less expensive than CCSD(T), but in many cases, especially in the calculation of the hyperpolarizability, the inclusion of the triples might be quite important. From a computational point of view, MP2 is the most economical post-Hartree–Fock method available for a large spectrum of molecular systems. It is seen to be particularly successful in several classes of molecules.^{52–55}

The electron correlation correction (ECC) is defined as

$$\text{ECC} = \text{CCSD(T)} - \text{SCF} \quad (6)$$

TABLE 1: Basis Sets Used in This Work

basis set	system			
	O	H	He	CGTF
WHe1	[6s4p3d1f]	[4s3p]	[4s3p]	79
WHe2	[6s4p3d1f]	[4s3p1d]	[4s3p1d]	94
WHe3	[6s4p3d1f]	[4s3p1d]	[6s4p3d]	109
WHe4	[9s6p5d1f]	[6s5p2d]	[6s5p3d]	157
WHe5	[9s6p6d4f]	[6s5p3d2f]	[6s5p3d2f]	235
WHe6	[18s13p8d6f]	[12s8p5d]	[13s10p6d]	334
WHe7	[18s13p10d7f]	[12s8p5d]	[13s11p7d]	359
WHe8	[18s13p10d7f]	[12s8p5d1f]	[13s11p7d1f]	380
H ₂ O \cdots Ne				
O	H	Ne	CGTF	
WNe1	[6s4p3d1f]	[4s3p]	[7s5p4d1f]	115
WNe2	[6s4p3d1f]	[4s3p1d]	[7s5p4d1f]	125
WNe3	[9s6p5d1f]	[6s5p2d]	[7s5p4d1f]	170
WNe4	[9s6p5d4f]	[6s5p3d2f]	[7s5p5d3f]	253
H ₂ O \cdots Ar				
O	H	Ar	CGTF	
WAR1	[6s4p3d1f]	[4s3p]	[8s6p5d4f]	145
WAR2	[6s4p3d1f]	[4s3p1d]	[8s6p5d4f]	155
WAR3	[9s6p5d1f]	[6s5p2d]	[8s6p5d4f]	200
WAR4	[9s6p5d4f]	[6s5p3d2f]	[8s6p5d4f]	264
H ₂ O \cdots Kr				
O	H	Kr	CGTF	
WKR1	[6s4p3d1f]	[4s3p]	[8s7p6d5f]	160
WKR2	[6s4p3d1f]	[4s3p1d]	[8s7p6d5f]	170
WKR3	[9s6p5d1f]	[6s5p2d]	[8s7p6d5f]	215
WKR4	[9s6p5d4f]	[6s5p3d2f]	[8s7p6d5f]	279
H ₂ O \cdots Xe				
O	H	Xe	CGTF	
WXe1	[6s4p3d1f]	[4s3p]	[9s8p7d1f]	141
WXe2	[6s4p3d1f]	[4s3p1d]	[9s8p7d1f]	151
WXe3	[6s4p3d1f]	[4s3p1d]	[9s8p7d3f]	165
WXe4	[9s6p5d1f]	[6s5p2d]	[9s8p7d1f]	196
WXe5	[9s6p5d1f]	[6s5p2d]	[9s8p7d3f]	210
WXe6	[9s6p6d4f]	[6s5p3d2f]	[9s8p7d1f]	260
WXe7	[9s6p6d4f]	[6s5p3d2f]	[9s8p7d3f]	274
WXe8	[9s6p6d4f]	[6s5p3d2f]	[9s8p7d5f]	288

The interaction property $P_{\text{int}}(\text{A} \cdots \text{B})$ of two interacting subsystems A and B may be defined as

$$P_{\text{int}}(\text{A} \cdots \text{B}) = P(\text{A} \cdots \text{B}) - P(\text{A}) - P(\text{B}) \quad (7)$$

This definition should provide accurate estimates of the interaction properties if flexible, nearly saturated basis sets are used. In practice, we can use the counterpoise correction (CP) method⁵⁶ to eliminate basis set superposition errors (BSSEs) from the calculations of the interaction properties. In this spirit, we replace the above definition by

$$P_{\text{int}}(\text{A} \cdots \text{B}) = P(\text{A} \cdots \text{B}) - P(\text{A} \cdots \text{X}) - P(\text{X} \cdots \text{B}) \quad (8)$$

where $P(\text{A} \cdots \text{X})$ is the value of property P for subsystem A in the presence of the ghost orbitals of subsystem B.

TABLE 2: Description of the Basis Sets Used in This Work (Gaussian-Type Function Exponents in Parentheses)

system	basis set	CGTF	substrate	description
H ₂ O	[6s4p3d1f/4s3p] ^a	66	D95'(9s5p/4s)[4s2p/2s]	+O: s(0.086186, 0.02610), p(0.063684, 0.018978), d(1.0656, 0.1417, 0.0517), f(0.1417), +H: s(0.048273, 0.013121), p(0.7947, 0.1554, 0.0687)
	[6s4p3d1f/4s3p1d] ^a	76	D95'(9s5p/4s)[4s2p/2s]	+H: d(0.1554)
	[9s6p5d1f/6s5p2d] ^b	121	(12s7p/6s)[7s4p/4s]	+O: s(0.07733, 0.02874), p(0.05302, 0.01898), d(1.10388, 0.41154, 0.15343, 0.05720, 0.02133), f(0.15343) +H: s(0.031302, 0.010891), p(1.78194, 0.77904, 0.14890, 0.06510, 0.02846), d(0.77904, 0.14890)
	[9s6p6d4f/6s5p3d2f] ^b	185	(12s7p/6s)[7s4p/4s]	+O: d(2.96093), f(1.10388, 0.41154, 0.05720), +H: d(0.06510), f(0.77904, 0.14890)
	[18s13p8d6f/12s8p5d] ^b	261	(14s9p/9s)	+O: s(0.072459, 0.028849, 0.011486, 0.004573), p(0.046088, 0.018642, 0.00754, 0.00305), d(1.8040, 1.0930, 0.6622, 0.4012, 0.2431, 0.1473, 0.0541, 0.0199) +H: s(0.0280548, 0.0117535, 0.0049241), p(1.8303, 1.1948, 0.7799, 0.3323, 0.1416, 0.0603, 0.0257)
	[18s13p10d7f/12s8p5d] ^b	278	(14s9p/9s)	+O: d(2.9773, 0.0073), f(1.0930)
	[18s13p10d7f/12s8p5d1f] ^b	292	(14s9p/9s)	+H: f(0.1416)
	[4s3p] ^c	13	(4s)[2s]	+s(0.0714965, 0.0171556), p(1.1298, 0.2484, 0.0553)
	[4s3p1d] ^c	18	(4s)[2s]	+d(0.2484)
	[6s4p3d] ^d	33	(6s)[4s]	+s(0.06545, 0.02050), p(1.2508, 0.5523, 0.2439, 0.0810), d(0.5174, 0.1990, 0.0765)
He	[6s5p3d] ^d	36	(6s)[4s]	+p(0.0269)
	[6s5p3d2f] ^d	50	(6s)[4s]	+f(0.1990, 0.0765)
	[13s10p6d] ^d	73	(10s)	+s(0.055703, 0.022656, 0.009215), p(1.45193, 1.01713, 0.71253, 0.49916, 0.24496, 0.12675, 0.06558, 0.03393, 0.01756, 0.00908), d(0.503003, 0.312382, 0.1940, 0.074823, 0.028858, 0.011130)
	[13s11p7d] ^d	81	(10s)	+p(4.22336), d(1.304187)
	[13s11p7d1f] ^d	88	(10s)	+f(0.1940)
Ne	[7s5p4d1f] ^d	49	(11s6p)[5s3p]	+s(0.117300, 0.045516), p(0.084897, 0.027088), d(1.6009, 0.6997, 0.3058, 0.1252), f(0.2411)
Ar	[7s5p5d3f] ^d	68	(11s6p)[5s3p]	+d(0.0513), f(0.9840, 0.0648)
	[8s6p5d4f] ^d	79	(15s9p)[6s4p]	+s(0.065199232, 0.030783713), p(0.053331519, 0.018040405), d(1.525783, 0.739767, 0.1739, 0.040879, 0.009610), f(0.439614, 0.1545, 0.054298, 0.019083)
Kr	[8s7p6d5f] ^d	94	(17s13p6d)[6s5p2d]	+s(0.071236179, 0.026249164), p(0.043258686, 0.016174259), d(0.4008, 0.1344, 0.0451, 0.0151), f(0.341006, 0.205383, 0.1237, 0.044872, 0.016277)
Xe	[9s8p7d1f] ^e	75	(16s13p7d)[7s6p4d]	+s(0.0473367, 0.0186548), p(0.0304765, 0.0122057), d(0.2998, 0.1058, 0.0373), f(0.1002)
	[9s8p7d3f] ^e	89	(16s13p7d)[7s6p4d]	+f(0.3006, 0.0334)
	[9s8p7d5f] ^e	103	(16s13p7d)[7s6p4d]	+f(0.1736, 0.0193)

^a Reference 9. ^b Reference 8. ^c This work. ^d Reference 33. ^e Reference 36.

Computational Strategy

Basis Sets. The selection of suitable basis sets is an essential factor of success in electric property calculations.^{57–59} Considerable efforts are invested in the construction of improved quality basis sets for use in polarizability calculations.^{60–62} Previous experience has shown that for atoms,^{63,64} diatomics,^{65–67} triatomics,^{68,69} and small polyatomics^{70,71} or clusters^{72,73} are possible to design purpose-oriented basis sets for (hyper)polarizability calculations. In this work we rely on basis sets that have been tested on (hyper)polarizability calculations for the water molecule and rare gas atoms but also on interaction (hyper)polarizability calculations for related systems as the water dimer and the He, Ne, Ar, Kr, and Xe homodiatoms.

The basis sets used in this work are listed and described in Tables 1 and 2. Their composition reflects a computational philosophy presented in detail elsewhere (see, for instance, refs 42 and 43). The following substrates were used for the interacting subsystems:

H₂O: D95≡(9s5p/4s) contracted to [4s2p/2s],⁷⁴ (12s7p/6s)[7s4p/4s],⁷⁵ (14s9p/9s),⁷⁶ uncontracted; He: (4s)[2s],⁷⁷ (6s)[4s],⁷⁵ (10s);⁷⁶ Ne: (11s6p)[5s3p];⁷⁸ Ar: (15s9p)[6s4p];⁷⁸ Kr: (17s13p6d)[6s5p2d];⁷⁸ Xe: (16s13p7d)[7s6p4d].⁷⁹

Molecular Geometries. The geometries used in this work are shown in Figure 1. For all H₂O–Rg systems, the z is the C₂ axis of the H₂O subsystem with the center of mass of H₂O at the origin and the oxygen nucleus on the negative z axis. The experimental geometry⁸⁰ is used for H₂O with R_{OH} = 0.9572 Å and θ = 104.52° for the HOH angle. For H₂O–He we used the theoretical geometry of Calderoni et al.⁸¹ For H₂O–Ne and H₂O–Ar we adopted the theoretical values reported by Hodges et al.⁸² For the remaining H₂O–Kr and H₂O–Xe we fully explored the respective PES, with the rare gas atom always on the xz plane. All calculations were performed with the [6s4p3d1f/4s3p] basis set for the water molecule, and [8s7p6d5f] and [9s8p7d1f] for the krypton and xenon atoms, respectively, at the MP2(FULL) level of theory. For the construction of the H₂O–Kr PES we calculated the interaction energy E_{int} for 546 configurations. The PES minimum was located by spline interpolation in a two-dimensional (2D) grid of 177 points. In the case of H₂O–Xe we calculated E_{int} for 1008 configurations. The PES minimum was located by spline interpolation in a 2D grid of 165 points. The calculated parameters are 7.339 a₀ and 109.3° for Kr and 7.825 a₀ and 114.5° for Xe. The shape of the

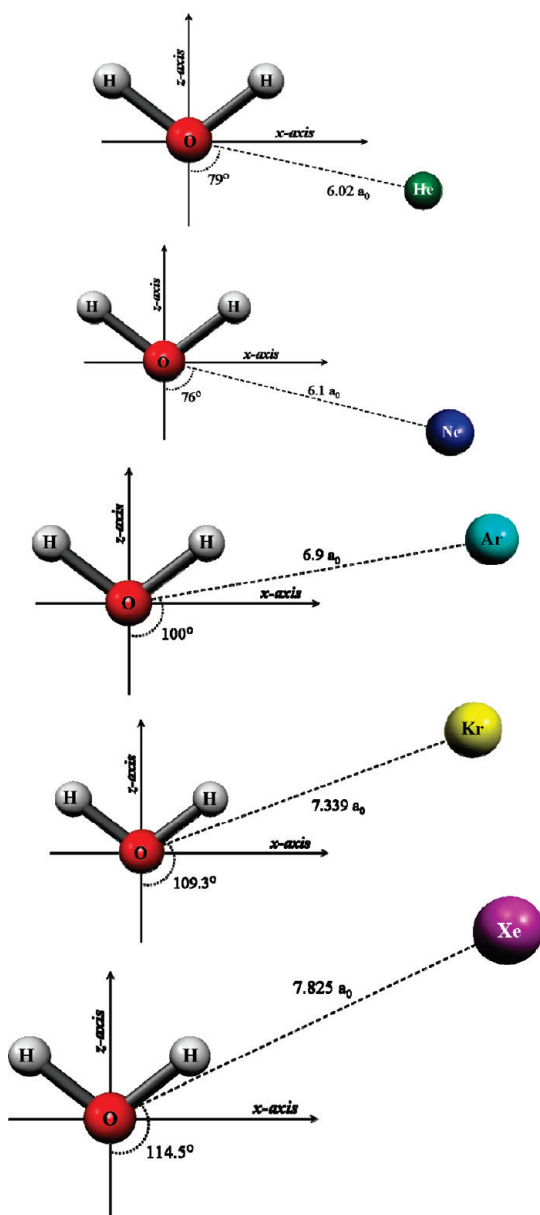


Figure 1. Equilibrium configuration of the H₂O–Rg complexes (see text for details).

PES is shown in Figures 2 and 3, for H₂O–Kr and H₂O–Xe, respectively.

Other Computational Details. Weak, homogeneous static electric fields of 0.005–0.03 $e^{-1}a_0^{-1}E_h$ were found to be suitable for the calculation of the electric properties. In all post-Hartree–Fock calculations, the 1, 2, 6, 10, and 19 innermost molecular orbitals (MOs) were kept frozen for H₂O–He, H₂O–Ne, H₂O–Ar, H₂O–Kr, and H₂O–Xe, respectively.

All calculations were performed with the Gaussian 98 program.⁸³

Unless otherwise specified, atomic units are used throughout this paper. Conversion factors to SI units are energy, 1 $E_h = 4.3597482 \times 10^{-18}$ J; length, 1 $a_0 = 0.529177249 \times 10^{-10}$ m; μ , 1 $ea_0 = 8.478358 \times 10^{-30}$ Cm; α , 1 $e^2a_0^2E_h^{-1} = 1.648778 \times 10^{-41}$ C² m² J⁻¹; β , 1 $e^3a_0^3E_h^{-2} = 3.206361 \times 10^{-53}$ C³ m³ J⁻²; and γ , 1 $e^4a_0^4E_h^{-3} = 6.235378 \times 10^{-65}$ C⁴ m⁴ J⁻³. Property values are mostly given as pure numbers, that is, μ/ea_0 , $\alpha/e^2a_0^2E_h^{-1}$, $\beta/e^3a_0^3E_h^{-2}$ and $\gamma/e^4a_0^4E_h^{-3}$.

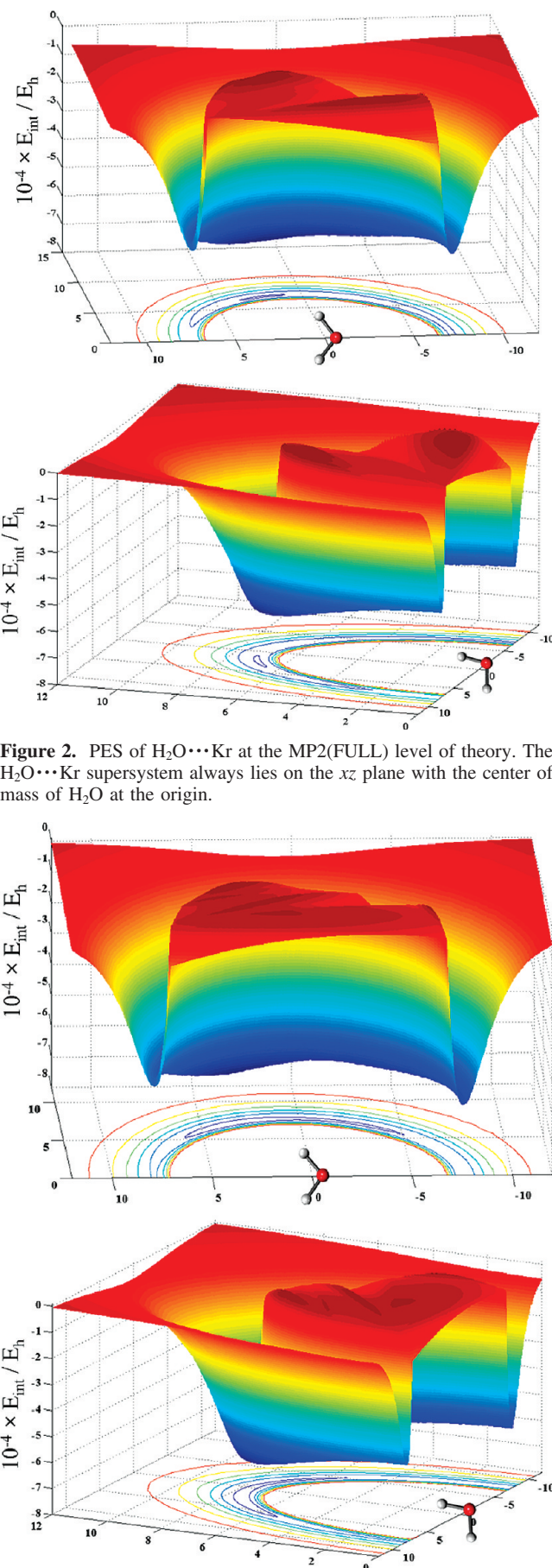


Figure 2. PES of H₂O...Kr at the MP2(FULL) level of theory. The H₂O...Kr supersystem always lies on the xz plane with the center of mass of H₂O at the origin.

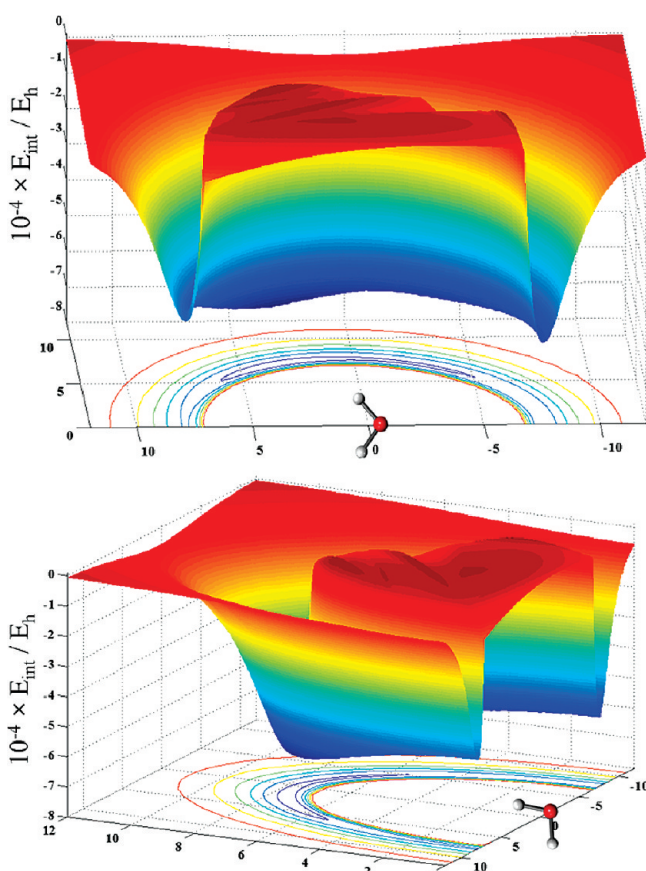


Figure 3. PES of H₂O...Xe at the MP2(FULL) level of theory. The H₂O...Xe supersystem always lies on the xz plane with the center of mass of H₂O at the origin.

TABLE 3: Interaction Electric Properties for the Equilibrium Configuration of the H₂O–He Complex

basis set	method	μ_x	μ_z	$\bar{\alpha}_{\text{int}}$	$\Delta\alpha_{\text{int}}$	$\bar{\beta}_{\text{int}}$	$\bar{\gamma}_{\text{int}}$
WHe1	SCF	0.0023	-0.0069	-0.0064	0.2863	0.53	-13.74
	MP2	0.0028	-0.0070	-0.0079	0.3311	0.80	-22.08
	MP4	0.0027	-0.0069	-0.0057	0.3415	0.79	-22.41
	CCSD	0.0025	-0.0070	-0.0047	0.3367	0.70	-18.84
	CCSD(T)	0.0026	-0.0069	-0.0044	0.3422	0.74	-19.88
	ECC	0.0003	0.0000	0.0020	0.0559	0.21	-6.14
WHe2	SCF	0.0023	-0.0068	-0.0064	0.2880	0.56	-14.01
	MP2	0.0028	-0.0070	-0.0070	0.3363	0.81	-22.14
	MP4	0.0026	-0.0070	-0.0043	0.3471	0.80	-22.40
	CCSD	0.0025	-0.0070	-0.0035	0.3422	0.70	-18.25
	CCSD(T)	0.0025	-0.0069	-0.0029	0.3481	0.73	-19.12
	ECC	0.0002	-0.0001	0.0035	0.0601	0.17	-5.11
WHe3	SCF	0.0023	-0.0068	-0.0067	0.2853	0.56	-14.19
	MP2	0.0027	-0.0069	-0.0072	0.3332	0.81	-22.26
	MP4	0.0025	-0.0069	-0.0044	0.3440	0.79	-22.07
	CCSD	0.0024	-0.0069	-0.0037	0.3389	0.69	-18.18
	CCSD(T)	0.0024	-0.0069	-0.0031	0.3448	0.72	-18.93
	ECC	0.0001	-0.0001	0.0036	0.0595	0.16	-4.74
WHe4	SCF	0.0023	-0.0067	-0.0068	0.2873	0.56	-14.09
	MP2	0.0027	-0.0069	-0.0068	0.3338	0.79	-21.61
	MP4	0.0025	-0.0069	-0.0040	0.3439	0.77	-21.23
	CCSD	0.0024	-0.0069	-0.0033	0.3381	0.68	-16.93
	CCSD(T)	0.0024	-0.0069	-0.0027	0.3442	0.71	-17.85
	ECC	0.0001	-0.0002	0.0041	0.0569	0.15	-3.76
WHe5	SCF	0.0023	-0.0067	-0.0069	0.2874	0.56	-14.07
	MP2	0.0026	-0.0069	-0.0064	0.3329	0.77	-21.05
WHe6	SCF	0.0023	-0.0067	-0.0068	0.2874	0.56	-14.03
	MP2	0.0026	-0.0069	-0.0065	0.3319	0.77	-21.10
WHe7	SCF	0.0023	-0.0067	-0.0068	0.2875	0.56	-14.03
	MP2	0.0026	-0.0069	-0.0065	0.3304	0.77	-20.78
WHe8	SCF	0.0023	-0.0067	-0.0068	0.2875	0.56	-14.02
	MP2	0.0026	-0.0069	-0.0063	0.3308	0.77	-20.09

TABLE 4: Interaction Electric Properties for the Equilibrium Configuration of the H₂O–Ne Complex

basis set	method	μ_x	μ_z	$\bar{\alpha}_{\text{int}}$	$\Delta\alpha_{\text{int}}$	$\bar{\beta}_{\text{int}}$	$\bar{\gamma}_{\text{int}}$
WNe1	SCF	0.0012	-0.0112	-0.0133	0.4785	0.79	-24.33
	MP2	0.0018	-0.0127	-0.0167	0.6126	1.28	-42.60
	MP4	0.0016	-0.0126	-0.0118	0.6280	1.32	-42.52
	CCSD	0.0015	-0.0121	-0.0112	0.6026	1.13	-36.12
	CCSD(T)	0.0016	-0.0122	-0.0097	0.6243	1.21	-37.54
	ECC	0.0004	-0.0010	0.0036	0.1458	0.42	-13.21
WNe2	SCF	0.0012	-0.0112	-0.0131	0.4797	0.79	-24.35
	MP2	0.0017	-0.0126	-0.0163	0.6146	1.27	-42.55
	MP4	0.0016	-0.0126	-0.0112	0.6301	1.32	-43.15
	CCSD	0.0015	-0.0121	-0.0107	0.6043	1.12	-36.29
	CCSD(T)	0.0016	-0.0122	-0.0091	0.6263	1.20	-37.78
	ECC	0.0004	-0.0010	0.0040	0.1466	0.41	-13.43
WNe3	SCF	0.0012	-0.0111	-0.0133	0.4832	0.78	-24.18
	MP2	0.0017	-0.0126	-0.0154	0.6165	1.24	-41.30
	MP4	0.0015	-0.0125	-0.0101	0.6312	1.27	-40.78
WeNe4	SCF	0.0012	-0.0111	-0.0133	0.4831	0.78	-24.02
	MP2	0.0015	-0.0126	-0.0145	0.6150	1.20	-39.69

Results and Discussion

The calculated values of the interaction electric properties for the equilibrium configuration of H₂O–Rg complexes are given in Tables 3–7 for He, Ne, Ar, Kr, and Xe, respectively. It should be noted here that the interaction dipole moment (μ_{int})

and polarizability (α_{int}) data are taken from another work.⁸⁴ Finally, in Table 8 we display some data for the geometry dependence of the interaction properties. This R-dependence of the properties is defined by the displacement of the Rg atom, without changing direction, around the equilibrium position.

TABLE 5: Interaction Electric Properties for the Equilibrium Configuration of the H₂O–Ar Complex

basis		μ_x	μ_z	$\bar{\alpha}_{\text{int}}$	$\Delta\alpha_{\text{int}}$	$\bar{\beta}_{\text{int}}$	$\bar{\gamma}_{\text{int}}$
WAr1	SCF	0.0470	-0.0214	0.0545	1.9891	4.28	-72.43
	MP2	0.0500	-0.0207	0.0672	2.3756	6.83	-106.51
	MP4	0.0495	-0.0204	0.0843	2.4205	7.17	-94.98
	CCSD	0.0488	-0.0204	0.0786	2.3340	6.46	-83.87
	CCSD(T)	0.0494	-0.0204	0.0891	2.4098	7.04	-79.87
	ECC	0.0024	0.0010	0.0346	0.4207	2.76	-7.44
WAr2	SCF	0.0469	-0.0214	0.0552	1.9912	4.28	-72.42
	MP2	0.0498	-0.0207	0.0688	2.3799	6.85	-105.83
	MP4	0.0494	-0.0204	0.0863	2.4248	7.18	-92.65
	CCSD	0.0487	-0.0204	0.0803	2.3367	6.45	-88.28
	CCSD(T)	0.0493	-0.0204	0.0910	2.4136	7.04	-83.16
	ECC	0.0024	0.0010	0.0358	0.4224	2.76	-10.74
WAr3	SCF	0.0468	-0.0212	0.0544	2.0014	4.24	-70.52
	MP2	0.0498	-0.0207	0.0713	2.3839	6.75	-98.65
	MP4	0.0495	-0.0205	0.0893	2.4247	7.08	-86.10
WAr4	SCF	0.0466	-0.0211	0.0535	2.0005	4.19	-70.13
	MP2	0.0498	-0.0208	0.0724	2.3775	6.69	-97.33

TABLE 6: Interaction Electric Properties for the Equilibrium Configuration of the H₂O–Kr Complex

basis		μ_x	μ_z	$\bar{\alpha}_{\text{int}}$	$\Delta\alpha_{\text{int}}$	$\bar{\beta}_{\text{int}}$	$\bar{\gamma}_{\text{int}}$
WKr1	SCF	0.0688	-0.0061	0.0900	2.6767	5.31	-125.91
	MP2	0.0717	-0.0037	0.1198	3.1829	9.29	-148.59
	MP4	0.0713	-0.0036	0.1429	3.2486	9.83	-131.61
	CCSD	0.0706	-0.0039	0.1332	3.1311	8.90	-116.49
	CCSD(T)	0.0712	-0.0037	0.1489	3.2296	9.78	-104.62
	ECC	0.0024	0.0024	0.0589	0.5529	4.47	21.29
WKr2	SCF	0.0688	-0.0061	0.0915	2.6805	5.34	-125.70
	MP2	0.0719	-0.0037	0.1230	3.1916	9.38	-146.96
	MP4	0.0714	-0.0036	0.1466	3.2575	9.91	-127.10
	CCSD	0.0707	-0.0039	0.1367	3.1376	8.96	-114.01
	CCSD(T)	0.0714	-0.0037	0.1527	3.2377	9.88	-102.92
	ECC	0.0026	0.0024	0.0611	0.5571	4.54	22.77
WKr3	SCF	0.0686	-0.0059	0.0908	2.6916	5.26	-123.16
	MP2	0.0719	-0.0036	0.1266	3.1955	9.30	-137.72
	MP4	0.0716	-0.0036	0.1507	3.2559	9.85	-113.90
WKr4	SCF	0.0684	-0.0059	0.0905	2.6915	5.20	-122.75
	MP2	0.0722	-0.0037	0.1288	3.1905	9.26	-134.41

The interaction properties for H₂O–He show remarkable stability at the SCF level of theory. Our reference SCF values are calculated with the very large WHe8 basis set and are $\mu_x = 0.0023$, $\mu_z = -0.0067$ for μ_{int} , $\bar{\alpha}_{\text{int}} = -0.0068$, $\Delta\alpha_{\text{int}} = 0.2875$, $\bar{\beta}_{\text{int}} = 0.56$, and $\bar{\gamma}_{\text{int}} = -14.02$. Our best ECC values are obtained with the WHe4 basis: $\mu_x = 0.0001$ and $\mu_z = -0.0002$ for μ_{int} , $\bar{\alpha}_{\text{int}} = 0.0041$, $\Delta\alpha_{\text{int}} = 0.0569$, $\bar{\beta}_{\text{int}} = 0.15$, and $\bar{\gamma}_{\text{int}} = -3.76$. Thus, the electron correlation effect is quite large for the polarizability and the hyperpolarizability. The magnitude of the mean polarizability decreases by 60.3%, while that of the anisotropy increases by 19.8%. The magnitude of the mean first hyperpolarizability increases by 26.8%. For the second hyperpolarizability, the ECC is negative and the magnitude of $\bar{\gamma}_{\text{int}}$ increases by 26.7%. The basis set dependence of $\bar{\gamma}_{\text{int}}$ for the sequence WHe1 \rightarrow WHe8 is illustrated in Figure 4. Clearly, the SCF values are very stable after WHe3. The MP2 and MP4 values are very close and the same is apparent for CCSD and CCSD(T). The CC values show significant relative change in WHe1 \rightarrow WHe4, but this change is small in absolute terms.

TABLE 7: Interaction Electric Properties for the Equilibrium Configuration of the H₂O–Xe Complex

basis		μ_x	μ_z	$\bar{\alpha}_{\text{int}}$	$\Delta\alpha_{\text{int}}$	$\bar{\beta}_{\text{int}}$	$\bar{\gamma}_{\text{int}}$
WXe1	SCF	0.0907	0.0049	0.1155	3.8066	6.74	-284.46
	MP2	0.0945	0.0090	0.1687	4.5581	13.65	-288.24
	MP4	0.0945	0.0091	0.2019	4.6793	14.87	-250.50
	CCSD	0.0938	0.0084	0.1880	4.5114	13.70	-233.93
	CCSD(T)	0.0948	0.0090	0.2128	4.6654	15.38	-205.97
	ECC	0.0041	0.0041	0.0973	0.8588	8.64	78.49
WXe2	SCF	0.0908	0.0049	0.1176	3.8114	6.68	-286.83
	MP2	0.0950	0.0091	0.1747	4.5760	13.75	-288.07
	MP4	0.0951	0.0092	0.2089	4.6988	15.02	-232.39
	CCSD	0.0943	0.0086	0.1945	4.5266	13.78	-236.12
	CCSD(T)	0.0954	0.0092	0.2200	4.6840	15.52	-206.45
	ECC	0.0046	0.0043	0.1024	0.8726	8.84	80.38
WXe3	SCF	0.0909	0.0050	0.1190	3.8131	6.70	-322.96
	MP2	0.0949	0.0092	0.1837	4.5552	13.60	-310.17
	MP4	0.0944	0.0093	0.2171	4.6546	14.66	-272.03
WXe4	SCF	0.0905	0.0051	0.1175	3.8260	6.56	-286.37
	MP2	0.0951	0.0092	0.1817	4.5857	13.75	-276.42
	MP4	0.0955	0.0094	0.2167	4.7016	15.08	-220.77
WXe5	SCF	0.0906	0.0051	0.1186	3.8280	6.56	-316.00
	MP2	0.0949	0.0093	0.1900	4.5635	13.58	-293.30
	MP4	0.0947	0.0093	0.2239	4.6557	14.72	-245.12
WXe6	SCF	0.0901	0.0051	0.1173	3.8242	6.45	-291.40
	MP2	0.0957	0.0093	0.1865	4.5839	13.81	-278.03
WXe7	SCF	0.0902	0.0051	0.1183	3.8269	6.46	-316.10
	MP2	0.0954	0.0093	0.1935	4.5596	13.66	-289.57
WXe8	SCF	0.0902	0.0051	0.1183	3.8271	6.47	-316.42
	MP2	0.0953	0.0093	0.1937	4.5534	13.67	-288.02

For H₂O–Ne basis set, WNe4 yields the best SCF values: $\mu_x = 0.0012$ and $\mu_z = -0.0111$ for μ_{int} , $\bar{\alpha}_{\text{int}} = -0.0133$, $\Delta\alpha_{\text{int}} = 0.4831$, $\bar{\beta}_{\text{int}} = 0.78$, and $\bar{\gamma}_{\text{int}} = -24.02$. We obtain very stable values at this level of theory. The most important changes are observed for $\Delta\alpha_{\text{int}}$ and $\bar{\gamma}_{\text{int}}$ but do not exceed $\sim 1\%$. Electron correlation has a small effect, in absolute terms, on the interaction dipole moment. The WNe2 basis yields CCSD(T) values of $\alpha_{\text{int}} = -0.0091$ and $\Delta\alpha_{\text{int}} = 0.6263$, $\bar{\beta}_{\text{int}} = 1.20$, and $\bar{\gamma}_{\text{int}} = -37.78$. We observe a strong decrease of the magnitude of the SCF value of the mean $\bar{\alpha}_{\text{int}}$ by 30.5%, while the magnitude of the SCF values of $\Delta\alpha_{\text{int}}$, $\bar{\beta}_{\text{int}}$, and $\bar{\gamma}_{\text{int}}$ increases by 30.6, 51.9, and 55.2%, respectively.

Our best SCF values for H₂O–Ar are calculated with the WAr4 basis set: $\mu_x = 0.0466$, $\mu_z = -0.0211$ for μ_{int} , $\bar{\alpha}_{\text{int}} = 0.0535$, $\Delta\alpha_{\text{int}} = 2.0005$, $\bar{\beta}_{\text{int}} = 4.19$, and $\bar{\gamma}_{\text{int}} = -70.13$. The SCF value of $\bar{\alpha}_{\text{int}}$ for H₂O–Ar is positive, while a negative one was observed for H₂O–He and H₂O–Ne. Electron correlation has a strong effect on the SCF values. Basis WAr2 yields CCSD(T) values of $\mu_x = 0.0493$ and $\mu_z = -0.0204$ or an increase by 5.1 and 4.7%, respectively. For the invariants of the dipole polarizability, the increase is 64.9 and 21.2% for $\bar{\alpha}_{\text{int}}$ and $\Delta\alpha_{\text{int}}$, respectively. For the hyperpolarizability, we observe changes of 64.5 and 14.8 for the magnitude of $\bar{\beta}_{\text{int}}$ and $\bar{\gamma}_{\text{int}}$, respectively. The MP2 method clearly overestimates the magnitude of the electron correlation effect for $\bar{\gamma}_{\text{int}}$.

For H₂O–Kr, at the SCF/WKr4 level of theory we observe the same signs for all properties as for H₂O–Ar at the analogous SCF/WAr4. SCF/WKr4 yields $\mu_x = 0.0684$ and $\mu_z = -0.0059$ for μ_{int} , $\bar{\alpha}_{\text{int}} = 0.0905$, $\Delta\alpha_{\text{int}} = 2.6915$, $\bar{\beta}_{\text{int}} = 5.20$ and $\bar{\gamma}_{\text{int}} =$

TABLE 8: Geometry Dependence (dP_{int}/dR_e) of the Electric Properties of the $\text{H}_2\text{O}\cdots\text{Rg}$ Complexes around the Equilibrium Position (See Text for Details)

property	$\text{H}_2\text{O}\cdots\text{He}^a$	$\text{H}_2\text{O}\cdots\text{Ne}^a$	$\text{H}_2\text{O}\cdots\text{Ar}^a$	$\text{H}_2\text{O}\cdots\text{Kr}^b$	$\text{H}_2\text{O}\cdots\text{Xe}^b$
$(d\mu_x/dR)_e$	-0.0028	-0.0035	-0.0287	-0.0360	-0.0410
$(d\mu_z/dR)_e$	0.0040	0.0071	0.0080	-0.0014	-0.0070
$(d\bar{\alpha}/dR)_e$	0.0137	0.0278	0.0019	-0.0144	-0.0015
$(d\Delta\alpha/dR)_e$	-0.1344	-0.2227	-0.9465	-1.2440	-1.6530
$(d\beta/dR)_e$	-0.83	-1.44	-2.81	-1.36	3.80
$(d\bar{\gamma}/dR)_e$	9.89	25.42	73.71	144.71	324.68

^a CCSD(T) values. ^b MP4 values.

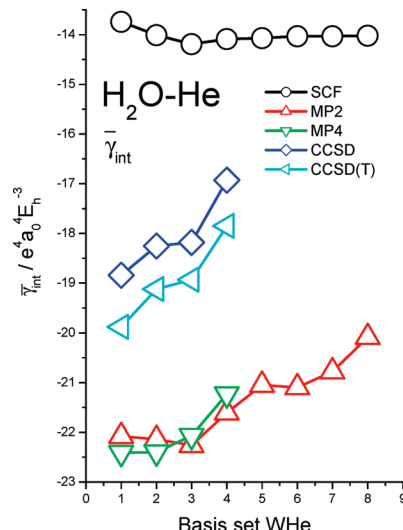


Figure 4. Basis set dependence of the interaction mean second hyperpolarizability $\bar{\gamma}_{\text{int}}$ of $\text{H}_2\text{O}-\text{He}$.

-122.75. As was the case for $\text{H}_2\text{O}-\text{Ar}$, for $\text{H}_2\text{O}-\text{Kr}$, $|\mu_x| > |\mu_z|$. Turning our attention to electron correlation effects, we observe a similar pattern for the interaction dipole moment and polarizability as in the case of $\text{H}_2\text{O}-\text{Ar}$. The CCSD(T)/WKR2 values of the interaction dipole moment are $\mu_x = 0.0714$ and $\mu_z = -0.0037$, or an increase of magnitude by 3.8% for μ_x and a reduction of 39.3% for μ_z . A uniform change is visible for the invariants of the polarizability, as CCSD(T)/WKR2 yields $\bar{\alpha}_{\text{int}} = 0.1527$ and $\Delta\alpha_{\text{int}} = 3.2377$, 66.8 and 20.8%, respectively, above the SCF values. For $\bar{\beta}_{\text{int}}$, the CCSD(T)/WKR2 value is 9.88, an impressive 85.0% above the SCF value of 5.34. Again, the MP2 method clearly overestimates the magnitude of the electron correlation effect for $\bar{\gamma}_{\text{int}}$. We observe, for the first time, that CCSD(T) reduces the magnitude of $\bar{\gamma}_{\text{int}}$ by 18.1%.

We employed eight basis sets in total for the calculation of the interaction properties of the $\text{H}_2\text{O}-\text{Xe}$ complex. With the notable exception of the second hyperpolarizability, all calculated interaction properties are positive at the SCF level. The WXe8 basis set yields SCF values of $\mu_x = 0.0902$ and $\mu_z = 0.0051$ for μ_{int} , $\alpha_{\text{int}} = 0.1183$, $\Delta\alpha_{\text{int}} = 3.8271$, $\bar{\beta}_{\text{int}} = 6.47$, and $\bar{\gamma}_{\text{int}} = -316.42$. The electron correlation effect is uniformly positive at the CCSD(T)/WXe2 level of theory. We obtain (SCF values in parentheses) $\mu_x = 0.0954$ (0.0908) and $\mu_z = 0.0092$ (0.0049) for μ_{int} , $\bar{\alpha}_{\text{int}} = 0.2200$ (0.1176), $\Delta\alpha_{\text{int}} = 4.6840$ (3.8114), $\bar{\beta}_{\text{int}} = 15.52$ (6.68) and $\bar{\gamma}_{\text{int}} = -206.45$ (-286.83), or an increase of the SCF value by 5.1, 87.8, 87.1, 22.9, 132.3, and 28.0%, respectively. The effect is quite strong for some of the interaction properties. In Figure 5 we have traced the performance of the sequence WXe1 → WXe8 in the calculation of $\bar{\gamma}_{\text{int}}$ for various levels of theory. We expect basis sets WXe7 and WXe8 to provide reliable SCF and MP2 values for $\bar{\gamma}_{\text{int}}$. At higher levels, the CCSD(T)/WXe1 and CCSD(T)/WXe2 values are sufficiently close to MP4/WXe2 and MP4/WXe4.

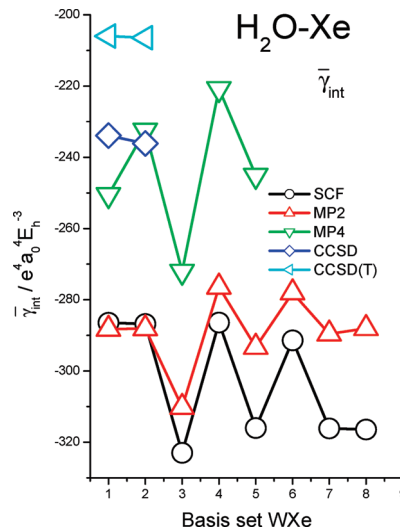


Figure 5. Basis set dependence of the interaction mean second hyperpolarizability $\bar{\gamma}_{\text{int}}$ of $\text{H}_2\text{O}-\text{Xe}$.

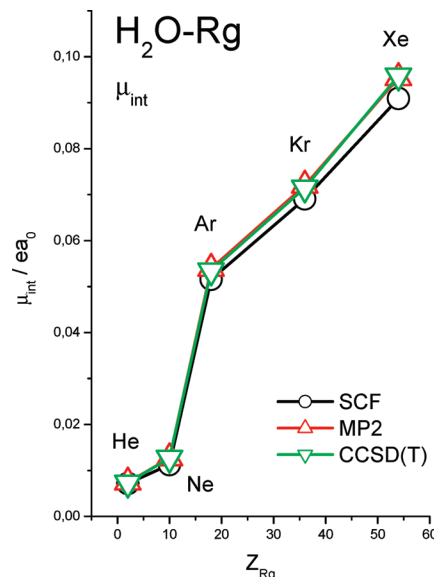


Figure 6. Interaction dipole moment $\bar{\mu}_{\text{int}}$ for the equilibrium configuration of $\text{H}_2\text{O}-\text{Rg}$.

In Figures 6–10 we present collective results for the evolution of the interaction properties. We show only SCF, MP2, and CCSD(T) values here. The basis sets used for the calculations are WHe3, WNe2, WAr2, WKR2, and WXe2. In Figure 6 we plot the total interaction dipole moment (see eq 2) as function of the atomic number Z_{Rg} . Clearly, all methods are in close agreement in reproducing the evolution of $\bar{\mu}_{\text{int}}$ with Z_{Rg} . Figure 7 shows that $\alpha_{\text{int}}(\text{H}_2\text{O}-\text{He}) > \bar{\alpha}_{\text{int}}(\text{H}_2\text{O}-\text{Ne})$. The ECC increases very strongly after $\text{H}_2\text{O}-\text{Ne}$. It is worth noting that the SCF curve differs strongly from the CCSD(T) one as Z_{Rg} increases.

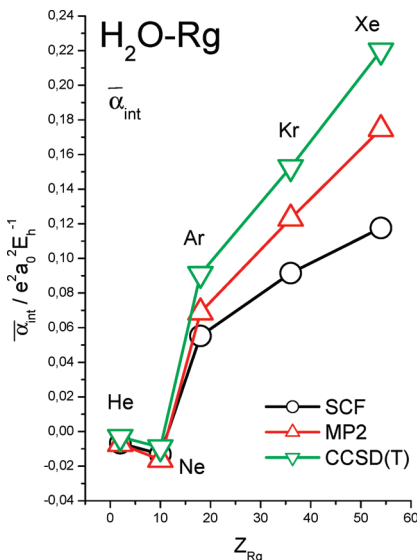


Figure 7. Interaction mean polarizability $\bar{\alpha}_{\text{int}}$ for the equilibrium configuration of H₂O–Rg.

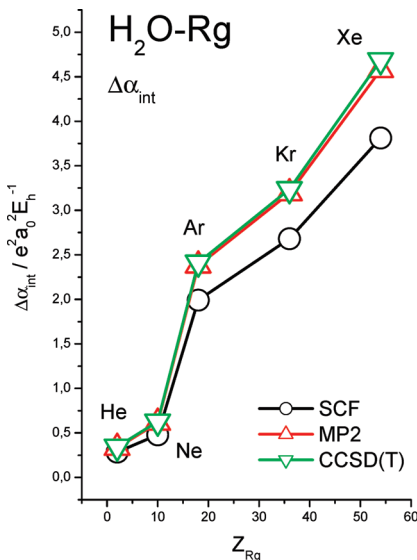


Figure 8. Interaction polarizability anisotropy $\Delta\bar{\alpha}_{\text{int}}$ for the equilibrium configuration of H₂O–Rg.

Figure 8 reveals that the dependence of $\Delta\bar{\alpha}_{\text{int}}$ on Z_{Rg} closely resembles that of μ_{int} . Moreover, the MP2 and CCSD(T) curves are very similar. In Figure 9 we show that the first hyperpolarizability $\bar{\beta}_{\text{int}}$ increases more strongly at the MP2 and CCSD(T) than at the SCF level of theory. Again, we observe a very strong dependence of the ECC on the atomic number of the rare gas atom. Finally, Figure 10 shows that, for $\bar{\gamma}_{\text{int}}$, the evolutions of SCF and MP2 are quite similar. The ECC becomes positive after H₂O–Ar.

In Figures 11 (H₂O–He), 12 (H₂O–Ne), 13 (H₂O–Ar), 14 (H₂O–Kr), and 15 (H₂O–Xe), we show the R-dependence of the interaction electric properties as the Rg atoms is displaced around the respective equilibrium position. We performed calculations at $(R - R_e)/a_0 = \pm 0.2, \pm 0.4, \pm 0.6$, and ± 0.8 . For H₂O–Rg, Rg = He, Ne, and Ar, we report values at the SCF, MP2, and CCSD(T) levels of theory. For the large systems H₂O–Rg, Rg = Kr and Xe, we report values at the SCF, MP2, and MP4 levels of theory. The basis sets used in this part of our work are WHe1, WNe1, WAr1, WKr1 and WXe1. Figures 11–15 offer valuable information on the shape of the R-

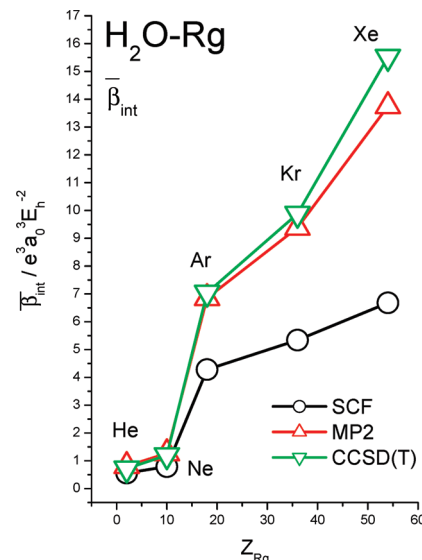


Figure 9. Interaction mean first hyperpolarizability $\bar{\beta}_{\text{int}}$ for the equilibrium configuration of H₂O–Rg.

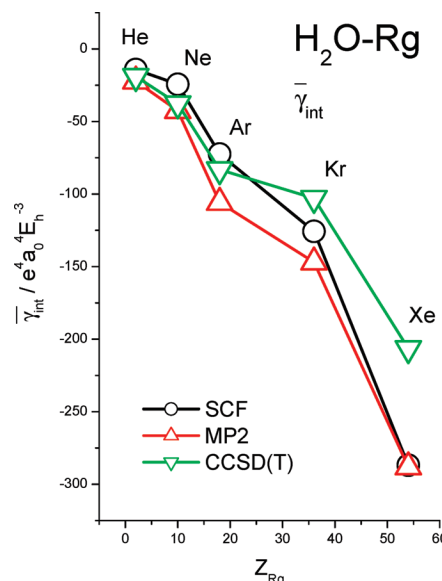


Figure 10. Interaction mean second hyperpolarizability $\bar{\gamma}_{\text{int}}$ for the equilibrium configuration of H₂O–Rg.

dependence curves around the equilibrium geometry of the complexes H₂O–Rg. In Table 8 we have collected the derivatives $(dP_{\text{int}}/dR)_e$, calculated at the highest level of theory used for each system. Interesting patterns appear for some properties. For μ_x , $\Delta\bar{\alpha}_{\text{int}}$, and $\bar{\gamma}_{\text{int}}$, the derivative increases monotonically for He → Ne → Ar → Kr → Xe.

Conclusions

We have reported an extensive investigation of the interaction (hyper)polarizability in the complexes H₂O–Rg, Rg = He, Ne, Ar, Kr, and Xe. All properties have been obtained from finite-field MP theory and CC calculations with large, flexible purpose-oriented basis sets. The interaction mean first hyperpolarizability is positive (SCF values in parentheses): $\bar{\beta}_{\text{int}}/e^3a_0^3E_h^{-2}$ (H₂O–Rg) = 0.72 (0.56), 1.20 (0.79), 7.04 (4.28), 9.88 (5.34), and 15.52 (6.68) for Rg = He, Ne, Ar, Kr, and Xe, respectively. For the interaction mean second hyperpolarizability, we have obtained (SCF values in parentheses): $\bar{\gamma}_{\text{int}}/e^4a_0^4E_h^{-3}$ (H₂O–Rg) = -18.93 (-14.19), -37.78 (-24.35), -83.16 (-72.42), -102.92

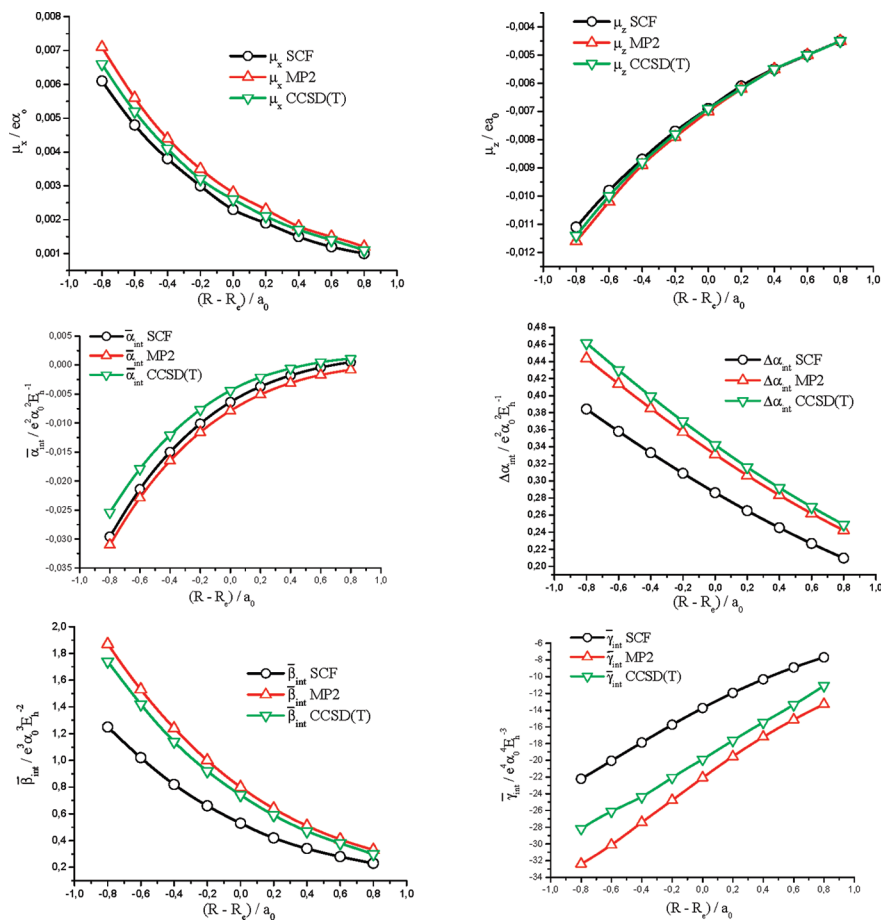


Figure 11. R-dependence of the interaction properties of $\text{H}_2\text{O}\cdots\text{He}$.

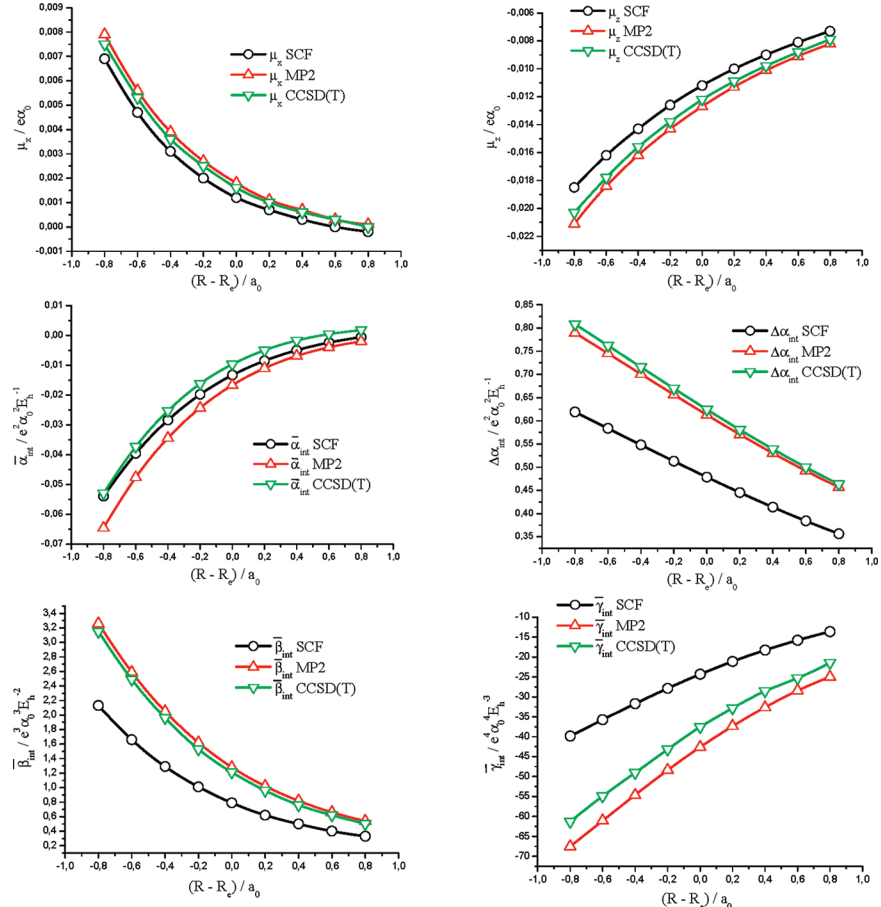
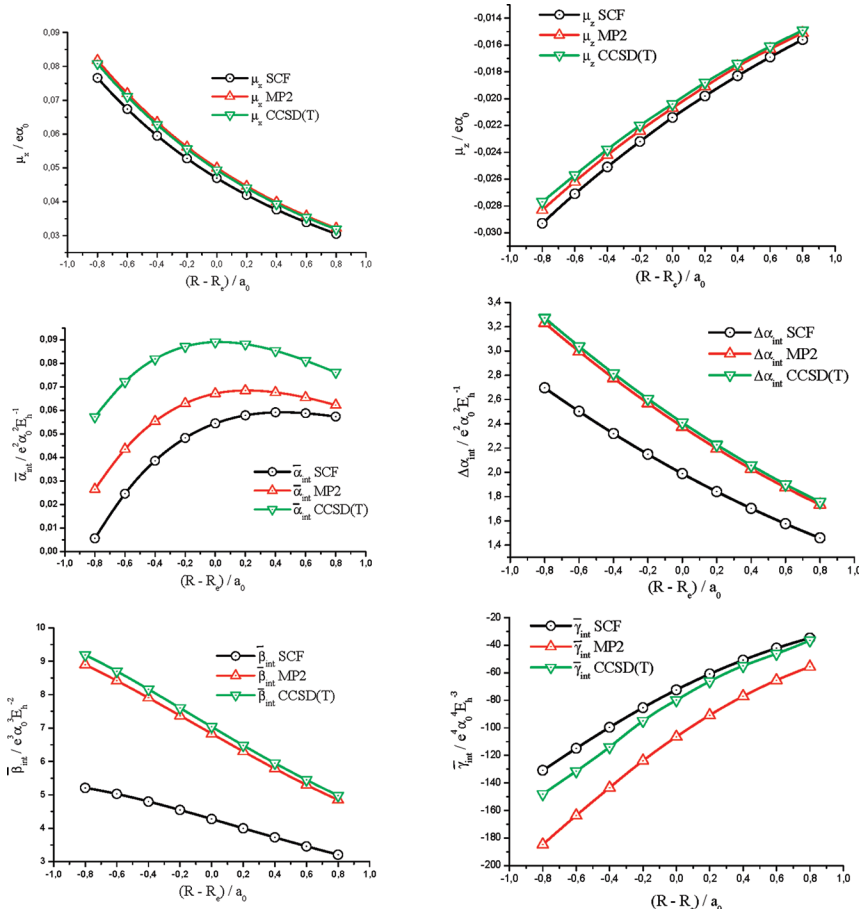
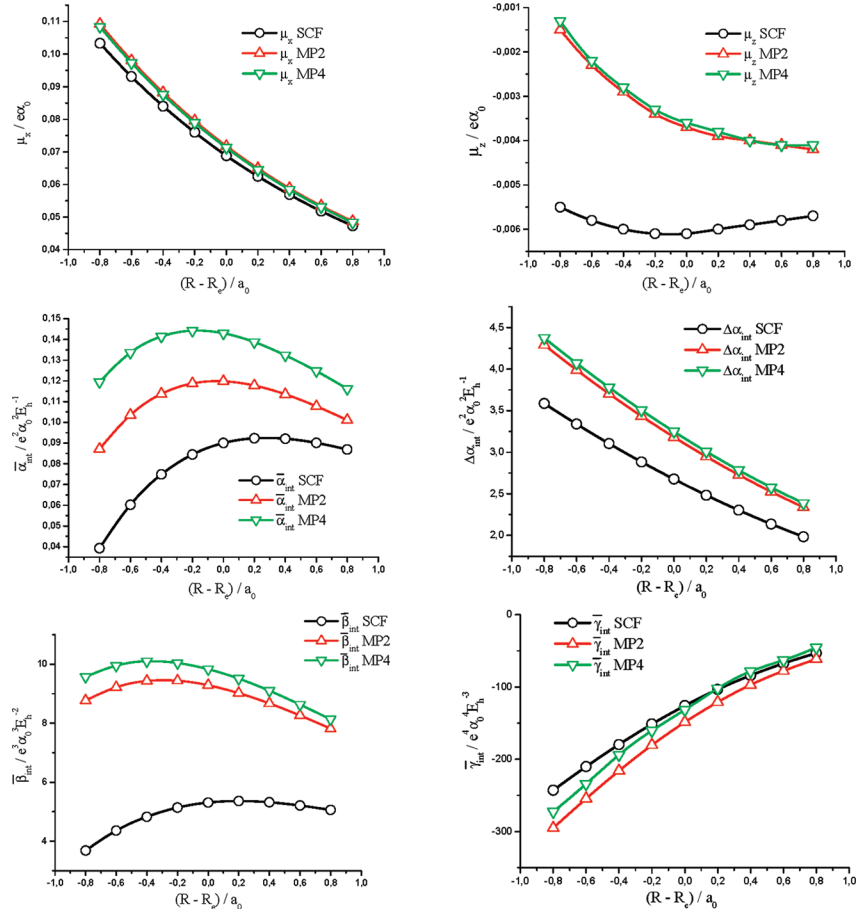


Figure 12. R-dependence of the interaction properties of $\text{H}_2\text{O}\cdots\text{Ne}$.

Figure 13. R -dependence of the interaction properties of H₂O \cdots Ar.Figure 14. R -dependence of the interaction properties of H₂O \cdots Kr.

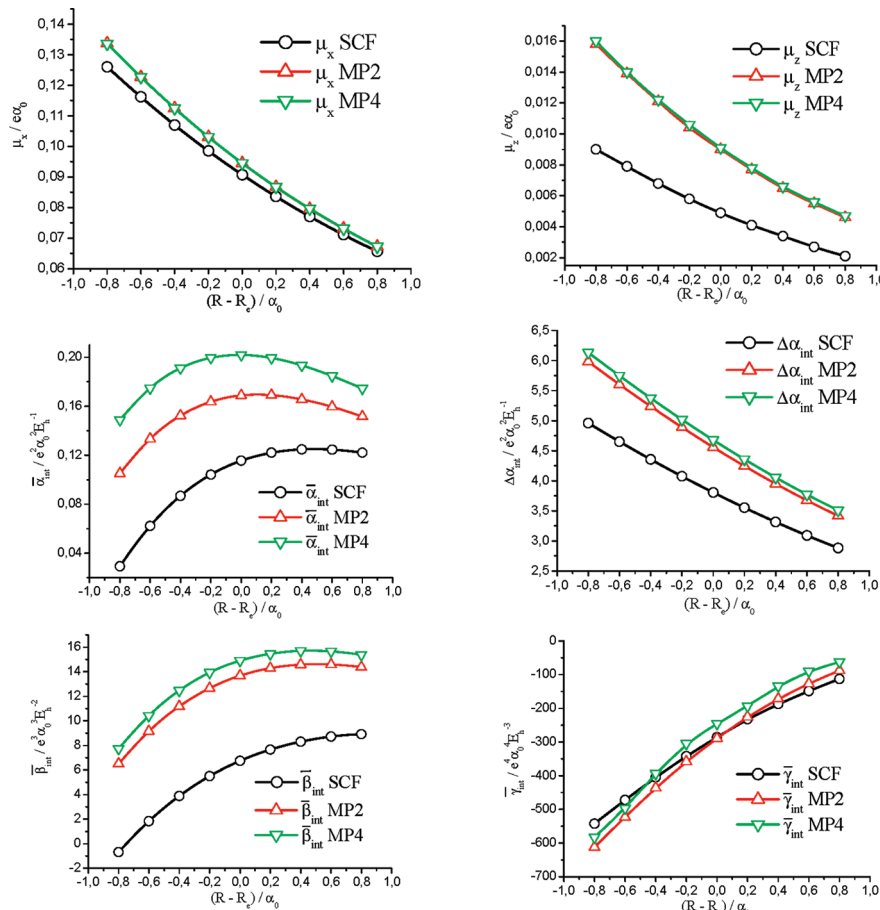


Figure 15. *R*-dependence of the interaction properties of $\text{H}_2\text{O}\cdots\text{Xe}$.

(−125.70), and −206.45 (−286.83) for $\text{Rg} = \text{He}, \text{Ne}, \text{Ar}, \text{Kr}$, and Xe . Basis set effects have been studied for all systems and at all levels of theory. We have also obtained important information for the dependence of the interaction properties on the displacement of the Rg atom around the equilibrium position for all systems.

References and Notes

- Su, J. T.; Xu, X.; Goddard, W. A. *J. Phys. Chem. A* **2004**, *108*, 10518.
- Lenz, A.; Ojamäe, L. *J. Mol. Struct.: THEOCHEM* **2010**, *944*, 163.
- Lenz, A.; Ojamäe, L. *J. Chem. Phys.* **2009**, *131*, 134302.
- Kazachenko, S.; Thakkar, A. J. *Chem. Phys. Lett.* **2009**, *476*, 120.
- Yu, H.; van Gunsteren, W. F. *J. Chem. Phys.* **2004**, *121*, 9549.
- Kunz, A. P. E.; van Gunsteren, W. F. *J. Phys. Chem. A* **2009**, *113*, 11570.
- Maroulis, G. *J. Chem. Phys.* **1991**, *94*, 1182.
- Maroulis, G. *Chem. Phys. Lett.* **1998**, *289*, 403.
- Maroulis, G. *J. Chem. Phys.* **2000**, *113*, 1813.
- Burham, C. J.; Li, J.; Xantheas, S. S.; Leslie, M. *J. Chem. Phys.* **1999**, *110*, 4566.
- Rodriguez, J.; Laria, D.; Marceca, E. J.; Estrin, D. A. *J. Chem. Phys.* **1999**, *110*, 9039.
- Lee, H. M.; Suh, S. B.; Lee, J. Y.; Tarakeshwar, P.; Kim, K. S. *J. Chem. Phys.* **2000**, *112*, 9759.
- Ghanty, T. K.; Ghosh, S. K. *J. Chem. Phys.* **2003**, *118*, 8547.
- Yang, S.; Senet, P.; van Alsenoy, C. *Int. J. Quantum Chem.* **2005**, *101*, 535.
- Hammond, J. R.; Govind, N.; Kowalski, K.; Autschbach, J.; Xantheas, S. S. *J. Chem. Phys.* **2009**, *131*, 214103.
- Batista, E. R.; Xantheas, S. S.; Jonsson, H. *J. Chem. Phys.* **1999**, *111*, 6011.
- Reis, H.; Raptis, S. G.; Papadopoulos, M. G. *Chem. Phys.* **2001**, *263*, 301.
- Delle Site, L.; Alavi, A.; Lynden-Bell, R. M. *Mol. Phys.* **1999**, *96*, 1683.
- Silvestrelli, P. L.; Parrinello, M. *Phys. Rev. Lett.* **1999**, *82*, 3308.
- Gubskaya, A. V.; Kusalik, P. G. *Mol. Phys.* **2001**, *99*, 1107.
- Jensen, L.; Swart, M.; van Duijnen, T.; Snijders, J. G. *J. Chem. Phys.* **2002**, *117*, 3316.
- Kongsted, J.; Osted, A.; Mikkelsen, K. V.; Christiansen, O. *J. Chem. Phys.* **2003**, *119*, 10519.
- Kongsted, J.; Osted, A.; Mikkelsen, K. V.; Christiansen, O. *J. Chem. Phys.* **2004**, *120*, 3787.
- Pyatt, R. D.; Shelton, D. P. *J. Chem. Phys.* **2001**, *114*, 9938.
- Tabisz, G. C.; Neuman, M. N., Eds.; *Collision-and Interaction-Induced Spectroscopy*; Kluwer: Dordrecht, The Netherlands, 1995.
- Birnbaum, G. *Phenomena Induced by Intermolecular Interactions*; Plenum: New York, 1985.
- Glaz, W.; Bancewicz, T. *J. Chem. Phys.* **2003**, *118*, 6264.
- Glaz, W.; Bancewicz, T.; Godet, J.-L. *J. Chem. Phys.* **2005**, *122*, 224323.
- Glaz, W.; Bancewicz, T.; Godet, J.-L.; Maroulis, G.; Haskopoulos, A. *Phys. Rev. A* **2006**, *73*, 042708.
- Maroulis, G.; Haskopoulos, A.; Glaz, W.; Bancewicz, T.; Godet, J.-L. *Chem. Phys. Lett.* **2006**, *428*, 28.
- Godet, J.-L.; Bancewicz, T.; Glaz, W.; Maroulis, G.; Haskopoulos, A. *J. Chem. Phys.* **2009**, *131*, 204305.
- Bancewicz, T.; Glaz, W.; Godet, J.-L.; Maroulis, G. *J. Chem. Phys.* **2008**, *129*, 124306.
- Baranowska, A.; Fernández, B.; Rizzo, A.; Jansík, B. *Phys. Chem. Chem. Phys.* **2009**, *11*, 9871.
- Cacheiro, J. L.; Fernández, B.; Rizzo, A.; Jansík, B.; Pedersen, T. B. *Mol. Phys.* **2008**, *106*, 881.
- Maroulis, G. *J. Phys. Chem. A* **2000**, *104*, 4772.
- Maroulis, G.; Haskopoulos, A. *Chem. Phys. Lett.* **2001**, *349*, 335.
- Maroulis, G.; Haskopoulos, A. *Chem. Phys. Lett.* **2002**, *358*, 64.
- Maroulis, G.; Haskopoulos, A.; Xenides, D. *Chem. Phys. Lett.* **2004**, *396*, 59.
- Haskopoulos, A.; Xenides, D.; Maroulis, G. *Chem. Phys.* **2005**, *309*, 271.
- Haskopoulos, A.; Maroulis, G. *Chem. Phys.* **2010**, *367*, 127.
- Cohen, H. D.; Roothaan, C. C. J. *J. Chem. Phys.* **1965**, *43*, S34.
- Maroulis, G. *J. Chem. Phys.* **1998**, *108*, 5432.
- Maroulis, G. *J. Chem. Phys.* **1999**, *111*, 583.
- Buckingham, A. D. *Adv. Chem. Phys.* **1967**, *12*, 107.

- (45) McLean, A. D.; Yoshimine, M. *J. Chem. Phys.* **1967**, *47*, 1927.
(46) Szabo, A.; Ostlund, N. S. *Modern Quantum Chemistry*; MacMillan: New York, 1982.
(47) Helgaker, T.; Jørgensen, P.; Olsen, J. *Molecular Electronic-Structure Theory*; Wiley: Chichester, U.K., 2000.
(48) Paldus, J.; Cizek, J. *Adv. Quantum Chem.* **1975**, *9*, 105.
(49) Bartlett, R. J. *Annu. Rev. Phys. Chem.* **1981**, *32*, 359.
(50) Urban, M.; Cernusak, I.; Kellö, V.; Noga, J. *Methods Comput. Chem.* **1987**, *1*, 117.
(51) Paldus, J.; Li, X. *Adv. Chem. Phys.* **1999**, *110*, 1.
(52) Xenides, D.; Maroulis, G. *Chem. Phys. Lett.* **2000**, *319*, 618.
(53) Maroulis, G. *J. Phys. B* **2001**, *34*, 3727.
(54) Maroulis, G. *Chem. Phys.* **2003**, *291*, 81.
(55) Xenides, D.; Maroulis, G. *J. Phys. B* **2006**, *39*, 3629.
(56) Boys, S. F.; Bernardi, F. *Mol. Phys.* **1970**, *19*, 55.
(57) Davidson, E. R.; Feller, D. *Chem. Rev.* **1986**, *86*, 681.
(58) Dykstra, C. E. *Ab Initio Calculation of the Structures and Properties of Molecules*; Elsevier: Amsterdam, 1988.
(59) Spackman, M. A. *J. Phys. Chem.* **1989**, *93*, 7594.
(60) Fantin, P. A.; Barbieri, P. L.; Canal Neto, A.; Jorge, F. E. *J. Mol. Struct.: THEOCHEM* **2007**, *810*, 103.
(61) Arruda, P. M.; Canal Neto, A.; Jorge, F. E. *Int. J. Quantum Chem.* **2009**, *109*, 1189.
(62) Baranowska, A.; Sadlej, A. J. *J. Comput. Chem.* **2010**, *31*, 552.
(63) Maroulis, G.; Bishop, D. M. *J. Phys. B* **1986**, *19*, 369.
(64) Goebel, D.; Hohm, U.; Maroulis, G. *Phys. Rev. A* **1996**, *54*, 1973.
(65) Maroulis, G.; Bishop, D. M. *Mol. Phys.* **1986**, *58*, 273.
(66) Maroulis, G.; Bishop, D. M. *Mol. Phys.* **1986**, *57*, 359.
(67) Maroulis, G. *J. Mol. Struct.: THEOCHEM* **2003**, *633*, 177.
(68) Maroulis, G. *Chem. Phys. Lett.* **1992**, *199*, 250.
(69) Maroulis, G. *Mol. Phys.* **2008**, *106*, 1517.
(70) Maroulis, G.; Thakkar, A. J. *J. Chem. Phys.* **1991**, *95*, 9060.
(71) Maroulis, G. *Chem. Phys. Lett.* **1996**, *259*, 654.
(72) Maroulis, G.; Xenides, D. *J. Phys. Chem. A* **1999**, *103*, 4590.
(73) Maroulis, G.; Pouchan, C. *J. Phys. Chem. B* **2003**, *107*, 10683.
(74) Dunning, T. H. *J. Chem. Phys.* **1970**, *53*, 2383.
(75) Thakkar, A. J.; Koga, T.; Saito, M.; Hoffmeyer, R. E. *Int. J. Quantum Chem.* **1993**, *S27*, 343.
(76) Partridge, H. Near Hartree-Fock quality Gaussian type orbital basis sets for the first- and third-row atoms. NASA Technical Memorandum 101044, **1989**.
(77) Van Duijneveldt, F. B. Gaussian basis sets for the atoms H-Ne for use in molecular calculations. RJ 945, IBM Research, **1971**.
(78) Schäfer, A.; Huber, C.; Ahlrichs, R. *J. Chem. Phys.* **1994**, *100*, 5829.
(79) Radzio, E.; Andzelm, J. *J. Comput. Chem.* **1987**, *8*, 117.
(80) Benedict, W. S.; Gailar, N.; Plyler, E. K. *J. Chem. Phys.* **1956**, *24*, 1139.
(81) Calderoni, G.; Cargnoni, F.; Raimondi, M. *Chem. Phys. Lett.* **2003**, *370*, 233.
(82) Hodges, M. P.; Wheatley, R. J.; Harvey, A. H. *J. Chem. Phys.* **2002**, *117*, 7169.
(83) Frisch, M. J.; Trucks, G. W.; Schlegel, H. B.; Scuseria, G. E.; Robb, M. A.; Cheeseman, J. R.; Zakrzewski, V. G.; Montgomery, J. A., Jr.; Stratmann, R. E.; Burant, J. C.; Dapprich, S.; Millam, J. M.; Daniels, A. D.; Kudin, K. N.; Strain, M. C.; Farkas, O.; Tomasi, J.; Barone, V.; Cossi, M.; Cammi, R.; Mennucci, B.; Pomelli, C.; Adamo, C.; Clifford, S.; Ochterski, J.; Petersson, G. A.; Ayala, P. Y.; Cui, Q.; Morokuma, K.; Malick, D. K.; Rabuck, A. D.; Raghavachari, K.; Foresman, J. B.; Cioslowski, J.; Ortiz, J. V.; Baboul, A. G.; Stefanov, B. B.; Liu, G.; Liashenko, A.; Piskorz, P.; Komaromi, I.; Gomperts, R.; Martin, R. L.; Fox, D. J.; Keith, T.; Al-Laham, M. A.; Peng, C. Y.; Nanayakkara, A.; Gonzalez, C.; Challacombe, M.; Gill, P. M. W.; Johnson, B. G.; Chen, W.; Wong, M. W.; Andres, J. L.; Head-Gordon, M.; Replogle, E. S.; Pople, J. A. *Gaussian 98*, revision A.7; Carnegie-Mellon Quantum Chemistry Publishing: Pittsburgh, PA, 1998.
(84) Haskopoulos, A.; Maroulis, G. To be submitted for publication.

JP101718S